Rashba effect in single-layer antimony telluroiodide SbTeI

Houlong L. Zhuang, Valentino R. Cooper, Haixuan Xu, P. Ganesh, Richard G. Hennig, and P. R. C. Kent

Phys. Rev. B **92**, 115302 — Published 4 September 2015

DOI: 10.1103/PhysRevB.92.115302

Rashba Effect in Single-Layer Antimony Telluroiodide SbTeI

Houlong L. Zhuang,[1,*] Valentino R. Cooper,[2] Haixuan Xu,[3] P. Ganesh,[1] Richard G. Hennig,[4] and P. R. C. Kent[5,1]

[1] *Center for Nanophase Materials Sciences, Oak Ridge National Laboratory, Bethel Valley Road, Oak Ridge, Tennessee 37831, United States*

[2] *Materials Science and Technology Division, Oak Ridge National Laboratory, Bethel Valley Road, Oak Ridge, Tennessee 37831, United States*

[3] *Department of Materials Science and Engineering, The University of Tennessee, Knoxville, Tennessee 37996, United States*

[4] *Department of Materials Science and Engineering, University of Florida, Gainesville, Florida 32611, United States*

[5] *Computer Science and Mathematics Division, Oak Ridge National Laboratory, Bethel Valley Road, Oak Ridge, Tennessee 37831, United States*

(Dated: June 24, 2015)

Exploring spin-orbit coupling (SOC) in single-layer materials is important for potential spintronics applications. Using first-principles calculations, we show that single-layer antimony telluroiodide, SbTeI, behaves as a two-dimensional semiconductor exhibiting a G_0W_0 bandgap of 1.82 eV. More importantly, we observe the Rashba spin-splitting in the SOC band structure of single-layer SbTeI with a sizable Rashba coupling parameter of 1.39 eV·Å, which is significantly larger than that of a number of two-dimensional systems including surfaces and interfaces. The low formation energy and real phonon modes of single-layer SbTeI imply that it is stable. Our study suggests that single-layer SbTeI is a candidate single-layer material for applications in spintronics devices.

I. INTRODUCTION

Spin-orbit coupling (SOC) leads to a wealth of fascinating physical phenomena.[1] One representative example is the Rashba effect, which demonstrates that Kramer's spin degeneracy is split due to SOC in an inversion-asymmetric material system. The Rashba effect can be utilized in important spintronics applications, such as the spin-based transistor by Datta and Das.[2]

One key ingredient for the occurrence of the Rashba effect is a broken inversion symmetry.[3] As a result, the Rashba effect is more commonly observed in two-dimensional (2D) systems including surfaces (e.g., Au(111) surface)[4] and interfaces (e.g., $LaAlO_3/SrTiO_3$ heterostructure)[5] than in bulk systems (*e.g.,* GeTe).[6] However, these 2D systems exhibit small Rashba coefficients typically ranging from 0.01 to 0.33 eV·Å.[3] Ultrathin 2D materials systems are commonly called single-layer materials. Research on single-layer materials is a fast developing field largely stimulated by the discovery of graphene a decade ago.[7] Since then various properties especially electrical and optical ones have been extensively studied.[8] In contrast, significantly fewer studies have reported the existence of the Rashba effect in single-layer materials,[9] although a variety of them such as ZnO[10] and GaSe[11] genuinely lack inversion symmetry. Therefore, searching for single-layer materials that display a sizable Rashba effect is of both scientific interest and practical importance.

The other crucial component for the Rashba effect is the presence of strong SOC. Since the strength of SOC sharply increases with atomic number, materials with a sufficiently large Rashba effect should contain heavy elements such as bismuth in the family of bismuth tellurohalides BiTeX (X = Cl, Br, and I).[12–14] This requirement also holds for single-layer materials, *e.g.,* single-layer BiTeI and BiTeBr have recently been predicted to exhibit the Rashba effect.[9]

In this paper, we follow a strategy of materials discovery by substituting the chemical element Bi in single-layer BiTeBr with another heavy element Sb in the same group. We show that single-layer SbTeI exhibits a low formation energy and is dynamically stable. More importantly, through relativistic first-principles calculations of band structures and spin textures, we predict that semiconducting single-layer SbTeI, similar to BiTeI, displays the Rashba effect with a sizable Rashba coefficient of 1.39 eV·Å, potentially useful for spintronics.

II. METHODS

We perform the first-principles calculations using the projector-augmented wave method as implemented in the plane-wave code VASP (version 5.3.3).[15–17] The effect of SOC is included using the second variation method.[18] For all calculations, a cutoff energy of 500 eV is used to expand the wavefunctions in plane waves, ensuring the convergence of the total energy to within 1 meV per formula unit. The density-functional theory (DFT) calculations employ the Perdew-Burke-Ernzerhof (PBE) exchange-correlation functional.[19] The k-point sampling uses the Monkhorst-Pack scheme[20] and employs a $15 \times 15 \times 1$ Γ-centered mesh for the DFT calculations and a Γ-centered $12 \times 12 \times 1$ grid for the more computationally demanding G_0W_0 calculations. A vacuum spacing of 20 Å reduces the interactions between the layers to a negligible level. All atoms in the simulation cells are relaxed until the forces are below 0.5 meV/Å. The G_0W_0 calculations are based on the PBE wavefunctions and use 128 bands

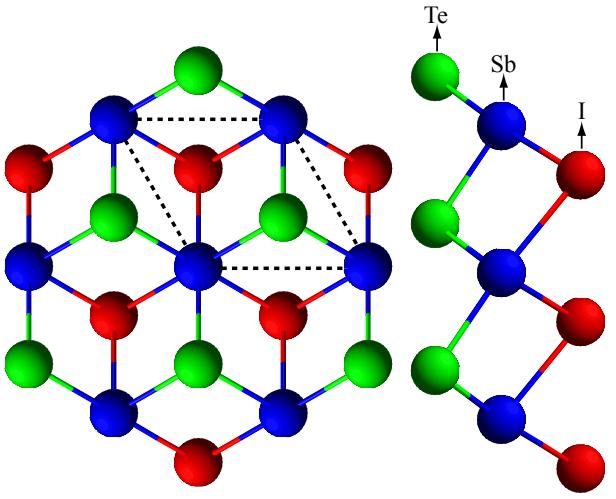

FIG. 1. Top and side view of the atomic structure of single-layer SbTeI. The unit cell is enclosed by dashed lines.

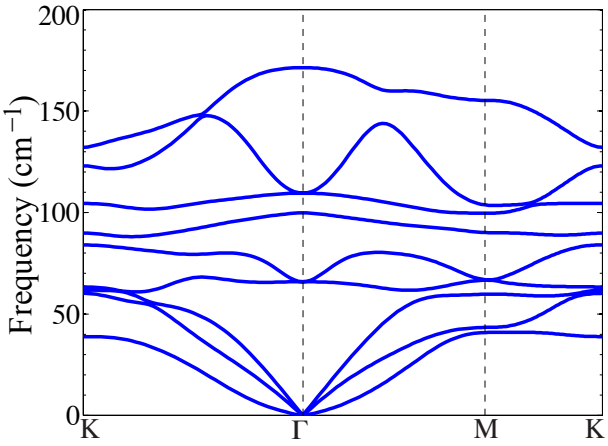

FIG. 2. Phonon spectrum of single-layer SbTeI.

and 96 frequency points to ensure that the quasiparticle bandgap is converged to 0.01 eV. For the phonon calculation, we use a $5 \times 5 \times 1$ supercell associated with a $3 \times 3 \times 1$ Γ-centered k-point mesh.

III. RESULTS AND DISCUSSION

We assume that single-layer SbTeI adopts the same hexagonal crystal structure as single-layer BiTeI, whose bulk counterpart has a trigonal structure with space group $P3m1$.[21] Figure 1 depicts the structure of single-layer SbTeI, which consists of three sublayers with the sixfold coordinated Sb atoms in the center sublayer bonded to the three-fold coordinated Te and I atoms located in the top and bottom sublayers. Additionally, the structure is similar to the $1T$ structure of several transition metal dichalcogenides such as TiS_2,[22] where the top and bottom sublayers are occupied by S atoms.

We employ two commonly used criteria to examine the stability of single-layer SbTeI.[23] First, we calculate the formation energy E_f of single-layer SbTeI with respect to the bulk structure using the formula $E_f = E_{2D} - E_{3D}$, where E_{2D} and E_{3D} are the energies of single-layer and bulk SbTeI, respectively. Bulk SbTeI is reported to have a monoclinic structure with space group $C12/m1$ (ICSD number: 31355).[24] Surprisingly, we find that bulk SbTeI with the same trigonal structure as bulk BiTeI exhibits an energy 19 meV/atom lower than monoclinic SbTeI. Taking into account the van der Waals interactions using the vdW-DF-optB88 functional,[25–28] the trigonal structure remains more stable than the monoclinic one by 16 meV/atom. In other words, we suggest that the ground-state structure of bulk SbTeI should be a trigonal one. Using the energy of this predicted ground state structure as a reference, we obtain E_f of 7 and 6 meV/atom with the PBE functional for single-layer SbTeI and BiTeI, respectively. Additionally, the vdW-DF-optB88 functional yields formation energies of 107 and 103 meV/atom for these two single-layer materials, respectively. Both formation energies are comparable to various single-layer materials such as transition-metal dichalcogenides with E_f ranging from 75 to 143 meV/atom,[29–31] implying that single-layer SbTeI and BiTeI can be synthesized.

Table I compares the calculated structural parameters of single-layer SbTeI and BiTeI.[21] As expected, the lattice constant, bond lengths, and bond angles of single-layer SbTeI are slightly smaller than those of single-layer BiTeI. Note that the calculated lattice constant of single-layer BiTeI agrees well with experimental in-plane lattice constant of bulk BiTeI of 4.34 Å.[21]

In addition to the test of formation energy, we calculate the phonon spectrum of single-layer SbTeI. Figure 2 shows that all phonon modes of SbTeI are real, confirming the dynamic stability of single-layer SbTeI.

Using the relaxed atomic configuration, we first investigate the electronic structures of single-layer SbTeI in the absence of SOC. Figure 3(a) shows the band structure calculated with the PBE functional. As can be seen, single-layer SbTeI is semiconducting with an indirect bandgap of 1.16 eV. The conduction band minimum (CBM) is located at the Γ point, while the two valence band maxima (VBM) are positioned slightly shifted away

TABLE I. Structural properties of of single-layer ATeI (A = Sb and Bi) calculated with the PBE functional. The lattice constant a_0 and bond lengths d are in Å, the bond angles Θ in degrees, and the formation energy E_f^{PBE} in meV/atom. The formation energy E_f^{vdW} calculated with the vdW-DF-optB88 functional is also shown for comparison.

	a_0	d_{A-Te}	d_{A-I}	Θ_{A-Te-A}	Θ_{A-I-A}	E_f^{PBE}	E_f^{vdW}
SbTeI	4.32	3.01	3.22	91.84	84.40	7	107
BiTeI	4.42	3.07	3.28	92.08	84.66	6	103

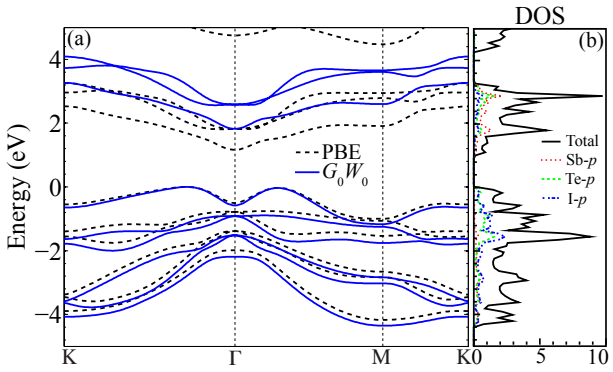

FIG. 3. (a) PBE and G_0W_0 band structures and (b) PBE density of states of single-layer SbTeI without SOC. The VBM is set to zero.

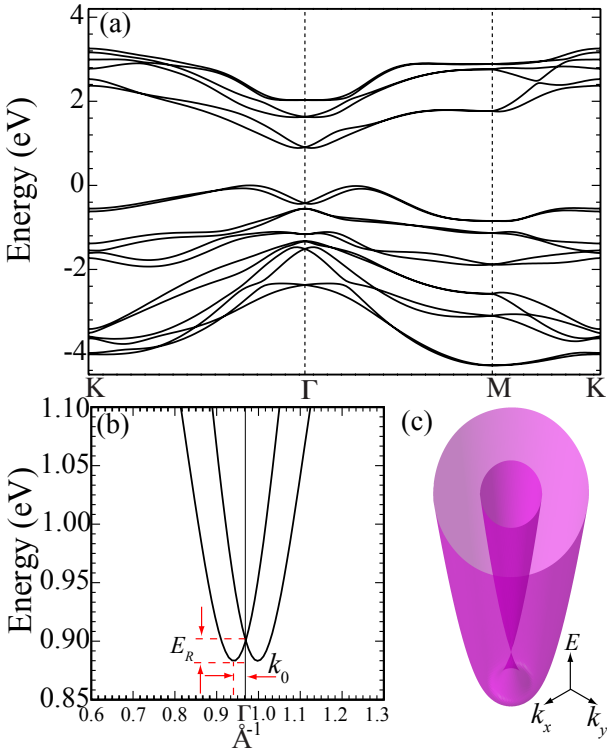

FIG. 4. (a) Band structure of single-layer SbTeI with SOC, (b) close-up view of the CBM around the Γ point, and (c) a three-dimensional sketch of the two CBM branches shown in (b).

from Γ along the $\Gamma \to K$ and $\Gamma \to M$ paths, respectively. The projected densities of states displayed in Fig. 3(b) show that in the energy window between −5.0 and 5.0 eV around the Fermi level, the electronic states are primarily composed of p orbitals from all three species.

To ameliorate the problem of bandgap underestimation with the PBE functional,[32] we calculate the quasiparticle energies using the many-body G_0W_0 approximation[33] and a Wannier function interpolation using the wannier90 code.[34–36] The orbital character for the initial projection of the Bloch states near the VBM and CBM onto the localized orbitals is obtained from the orbital-resolved density of states shown in Fig. 3(b) and consists of Sb p, Te p, and I p character. Then we obtain the full quasiparticle spectrum by interpolating the quasiparticle energies of a finite-size of k-point grid.[35,36] Figure 3(a) shows the interpolated quasiparticle energy spectrum, which in fact also simulates the spectrum that can be measured from angle-resolved photoemission spectroscopy (ARPES). We can see that the quasiparticle bandgap of single-layer SbTeI is increased to 1.82 eV from the PBE bandgap of 1.16 eV. This is similar to the gaps of other single-layer materials such as MoS_2 and WS_2.[37,38] Electronic and photovoltaic devices based on single-layer materials requires bandgaps within the visible light spectrum. Therefore, single-layer SbTeI could be another promising single-layer material useful for electronic devices and energy conversion applications.

Figure 4(a) shows that the SOC causes drastic changes in the electronic structure of single-layer SbTeI. First, a magnified view of the CBM near the Γ point in Fig. 4(b) and (c) unveils the most interesting feature: The initially degenerate bands split into two branches, hereafter referred to as inner and outer, respectively.[12] This is a signature indicator of the Rashba effect. Second, the SOC bandgap remains indirect, however, the band splitting reduces the bandgap from 1.16 to 0.87 eV. If we approximate the reduction of the quasiparticle bandgap due to the SOC by the reduction observed for the PBE functional of 0.29 eV, we can estimate the quasiparticle bandgap with SOC to be 1.53 eV.

To confirm that the splitting of the CBM at the Γ point in single-layer SbTeI is caused to the Rashba effect, we plot the spin texture of the inner and outer branches, which is proportional to the expectation value of the Pauli matrices $\langle\psi_{kn}|\hat{\sigma}|\psi_{kn}\rangle$. First of all, the spin texture shown in Fig. 5 illustrates that the inner branch exhibits a clockwise helicity, whereas the outer branch displays a counterclockwise helicity. Such a helicity crossover is another typical feature derived from the standard Rashba Hamiltonian.[1] In addition, the σ_x and σ_y spin components are both significantly larger than the σ_z one, indicating that the electronic states in single-layer SbTeI is mostly spin polarized in the xy-plane. This is similar to the case of the Te-terminated BiTeBr (0001) surface.[12]

Finally, we proceed to calculate the Rashba coefficient α_R, which describes the strength of the Rashba effect. The Rashba coefficient is given by $\alpha_R = 2E_R/k_0$, where E_R denoted in Fig. 4(b) is the Rashba energy and k_0 is the corresponding shift of crystal momentum. From Fig. 4(b), we estimate E_R, k_0, and α_R to be 17 meV, 0.024 Å^{-1}, and 1.39 eV·Å, respectively. Using the same methodology, we determine α_R for single-layer BiTeI as 1.97 eV·Å, consistent with the previously reported value of 1.86 eV·Å.[9] Although the α_R of single-layer SbTeI is somewhat smaller than that of single-layer BiTeI, it is competitive with several other materials such as the InGaAs/InAlAs heterostructure with a value of only

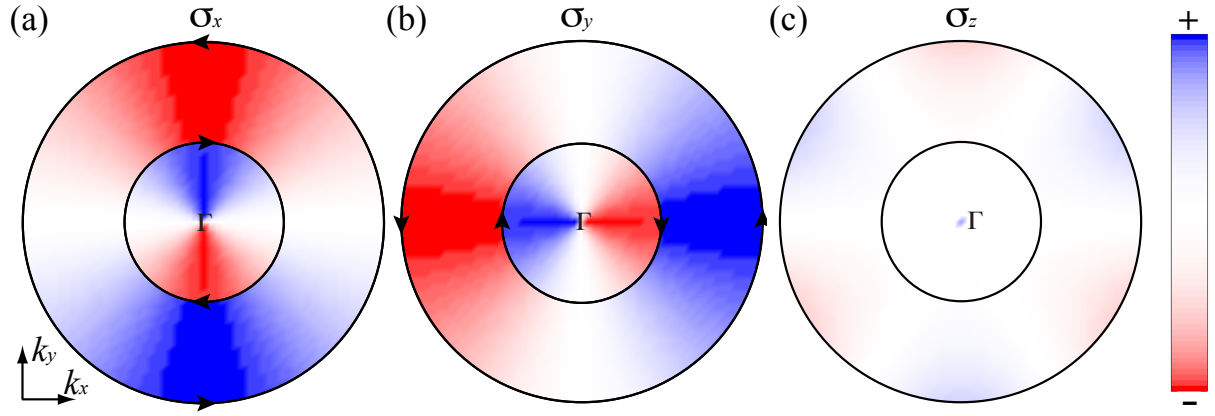

FIG. 5. Spin texture of single-layer SbTeI with spin polarizations along the (a) x, (b) y, and (c) z directions. The arrows are used to facilitate visualization of spin helicity of the inner and outer branches. The color bar denotes the components of spin polarizations ranging from negative (-) to positive (+).

0.07 eV·Å, which makes SbTeI another promising material for the spin-polarized field effect transistor.[39]

IV. CONCLUSIONS

In summary, we have predicted that single-layer SbTeI is a semiconductor with an indirect bandgap in PBE of 1.16 eV and in G_0W_0 of 1.82 eV. Spin-orbit coupling interactions reduces the bandgap by 0.29 eV. We show that including spin-orbit coupling interactions in the electronic structure calculation of single-layer SbTeI leads to a split and shift of the conduction band minimum, which is indicative of the Rashba effect. Calculations of the spin texture show a reversed spin helicity, confirming the Rashba effect. We find that SbTeI exhibits a sizable Rashba coefficient of 1.39 eV·Å. Although awaiting experimental confirmation, our work not only proposes an alternative single-layer material for spintronics applications but also manifests the importance of considering spin-orbit coupling in the study of a large number of emerging single-layer materials.

ACKNOWLEDGMENTS

Research sponsored by the Laboratory Directed Research and Development Program of Oak Ridge National Laboratory, managed by UT-Battelle, LLC, for the U. S. Department of Energy, and (HX) The University of Tennessee (UT) Science Alliance Joint Directed Research and Development Program (JDRD) and UT/ORNL Joint Institute of Advanced Materials (JIAM). RGH was supported by the NSF through CAREER award No. DMR-1056587. This research in part used computational resources of the Texas Advanced Computing Center under Contract No. TG-DMR140067. This research also used resources of the Oak Ridge Leadership Computing Facility at the Oak Ridge National Laboratory, which is supported by the Office of Science of the U.S. Department of Energy under Contract No. DE-AC05-00OR22725.

* zhuanghl@ornl.gov

[1] R. Winkler, *Spin-orbit Coupling Effects in Two-Dimensional Electron and Hole Systems* (Springer, 2003).
[2] S. Datta and B. Das, Applied Physics Letters **56**, 665 (1990).
[3] S. Picozzi, Frontiers in Physics **2** (2014), 10.3389/fphy.2014.00010.
[4] S. LaShell, B. A. McDougall, and E. Jensen, Phys. Rev. Lett. **77**, 3419 (1996).
[5] A. D. Caviglia, M. Gabay, S. Gariglio, N. Reyren, C. Cancellieri, and J.-M. Triscone, Phys. Rev. Lett. **104**, 126803 (2010).
[6] D. Di Sante, P. Barone, R. Bertacco, and S. Picozzi, Advanced Materials **25**, 509 (2013).
[7] K. S. Novoselov, D. Jiang, F. Schedin, T. J. Booth, V. V. Khotkevich, S. V. Morozov, and A. K. Geim, Proc. Nat. Acad. Sci. **102**, 10451 (2005).
[8] M. Xu, T. Liang, M. Shi, and H. Chen, Chem. Rev. **113**, 3766 (2013).
[9] Y. Ma, Y. Dai, W. Wei, X. Li, and B. Huang, Phys. Chem. Chem. Phys. **16**, 17603 (2014).
[10] C. Tusche, H. L. Meyerheim, and J. Kirschner, Phys. Rev. Lett. **99**, 026102 (2007).
[11] X. Li, M.-W. Lin, A. A. Puretzky, J. C. Idrobo, C. Ma, M. Chi, M. Yoon, C. M. Rouleau, I. I. Kravchenko, D. B. Geohegan, and K. Xiao, Scientific Reports **4**, 5497 (2014).
[12] S. V. Eremeev, I. P. Rusinov, I. A. Nechaev, and E. V. Chulkov, New Journal of Physics **15**, 075015 (2013).
[13] M. S. Bahramy, R. Arita, and N. Nagaosa, Phys. Rev. B

84, 041202 (2011).
[14] K. Ishizaka, M. S. Bahramy, H. Murakawa, M. Sakano, T. Shimojima, T. Sonobe, K. Koizumi, S. Shin, H. Miyahara, A. Kimura, K. Miyamoto, T. Okuda, H. Namatame, M. Taniguchi, R. Arita, N. Nagaosa, K. Kobayashi, Y. Murakami, R. Kumai, Y. Kaneko, Y. Onose, and Y. Tokura, Nature Mater. **10**, 521 (2011).
[15] G. Kresse and J. Furthmüller, Phys. Rev. B **54**, 11169 (1996).
[16] P. E. Blöchl, Phys. Rev. B **50**, 17953 (1994).
[17] G. Kresse and D. Joubert, Phys. Rev. B **59**, 1758 (1999).
[18] D. D. Koelling and B. N. Harmon, Journal of Physics C: Solid State Physics **10**, 3107 (1977).
[19] J. P. Perdew, K. Burke, and M. Ernzerhof, Phys. Rev. Lett. **77**, 3865 (1996).
[20] H. J. Monkhorst and J. D. Pack, Phys. Rev. B **13**, 5188 (1976).
[21] A. Shevelkov, E. Dikarev, R. Shpanchenko, and B. Popovkin, Journal of Solid State Chemistry **114**, 379 (1995).
[22] H. L. Zhuang and R. G. Hennig, The Journal of Physical Chemistry C **117**, 20440 (2013).
[23] H. L. Zhuang and R. G. Hennig, Journal of The Minerals, Metals & Materials Society (TMS) **66**, 366 (2014).
[24] G. Bergerhoff and I. D. Brown, in *Crystallographic Databases* (International Union of Crystallography, Chester, 1987).
[25] J. Klimeš, D. R. Bowler, and A. Michaelides, Journal of Physics: Condensed Matter **22**, 022201 (2010).
[26] M. Dion, H. Rydberg, E. Schröder, D. C. Langreth, and B. I. Lundqvist, Phys. Rev. Lett. **92**, 246401 (2004).
[27] G. Román-Pérez and J. M. Soler, Phys. Rev. Lett. **103**, 096102 (2009).
[28] T. Thonhauser, V. R. Cooper, S. Li, A. Puzder, P. Hyldgaard, and D. C. Langreth, Phys. Rev. B **76**, 125112 (2007).
[29] A. K. Singh, K. Mathew, H. L. Zhuang, and R. G. Hennig, The Journal of Physical Chemistry Letters **6**, 1087 (2015).
[30] H. L. Zhuang and R. G. Hennig, The Journal of Physical Chemistry C **117**, 20440 (2013).
[31] H. L. Zhuang, M. D. Johannes, M. N. Blonsky, and R. G. Hennig, Applied Physics Letters **104**, 022116 (2014).
[32] J. P. Perdew, Int. J. Quant. Chem. **30**, 451 (1986).
[33] M. Shishkin, M. Marsman, and G. Kresse, Phys. Rev. Lett. **99**, 246403 (2007).
[34] A. A. Mostofi, J. R. Yates, Y.-S. Lee, I. Souza, D. Vanderbilt, and N. Marzari, Computer Physics Communications **178**, 685 (2008).
[35] N. Marzari, A. A. Mostofi, J. R. Yates, I. Souza, and D. Vanderbilt, Rev. Mod. Phys. **84**, 1419 (2012).
[36] W. Ku, T. Berlijn, and C.-C. Lee, Phys. Rev. Lett. **104**, 216401 (2010).
[37] K. F. Mak, C. Lee, J. Hone, J. Shan, and T. F. Heinz, Phys. Rev. Lett. **105**, 136805 (2010).
[38] Q. H. Wang, K.-Z. Kourosh, A. Andras, J. N. Coleman, and M. S. Strano, Nature Nanotech. **7**, 699 (2012).
[39] J. Nitta, T. Akazaki, H. Takayanagi, and T. Enoki, Phys. Rev. Lett. **78**, 1335 (1997).